One-Step Synthesis and Structural Features of CdS/Montmorillonite Nanocomposites

Zhaohui Han,*,† Huaiyong Zhu,†,‡ Shaun R. Bulcock,† and Simon P. Ringer†

Australian Key Centre for Microscopy and Microanalysis, The University of Sydney, NSW 2006, Australia, and School of Chemistry, The University of Sydney, NSW 2006, Australia

Received: August 2, 2004; In Final Form: September 22, 2004

A novel synthesis method was introduced for the nanocomposites of cadmium sulfide and montmorillonite. This method features the combination of an ion exchange process and an in situ hydrothermal decomposition process of a complex precursor, which is simple in contrast to the conventional synthesis methods that comprise two separate steps for similar nanocomposite materials. Cadmium sulfide species in the composites exist in the forms of pillars and nanoparticles, the crystallized sulfide particles are in the hexagonal phase, and the sizes change when the amount of the complex for the synthesis is varied. Structural features of the nanocomposites are similar to those of the clay host but changed because of the introduction of the sulfide into the clay.

1. Introduction

Materials that incorporate one phase within another so as to generate a composite material are of significant and long-standing interest in the development of advanced materials with novel structures and modified properties. Nanocomposites provide further opportunities for synergizing properties between phases because the nanoscale dispersion of the second phase and the interface can elicit new functional properties.[1−3] The composites of CdS with various inorganic agents are examples that have received much attention. CdS itself is a semiconductor; besides possessing interesting optical properties,[4,5] the semiconductor is interesting for the special photocatalytic activity[6] and it is active under visible light for hydrogen production from water. It has been reported that supported CdS has a performance superior to that of unsupported CdS, because the active ingredient is dispersed on the supports, and the supports provide heterojunctions for electrons and holes that restrict the charge recombination.[7,8]

Selection of the matrix for composite materials containing CdS depends on the material's application. In recent work, CdS has been incorporated with mesoporous materials including SBA-15 silica,[9] MCM-41 silica,[10] and alumina,[11] producing size-confined CdS nanoparticles within the matrix materials. CdS also has been incorporated with porous alumina[12,13] and with layered metal oxides such as $KTiNbO_5$ and $K_2Ti_4O_9$,[7] producing catalysts for hydrogen production from water. In contrast, there has been relatively little research on the incorporation of CdS with a layered clay like montmorillonite, although layered clays have been intercalated with numerous oxide pillars in the last 25 years.[14,15] It has been reported that montmorillonite was pillared with chromium sulfide; the composite material was investigated as a catalyst for thiophene hydrodesulfurization.[16] In addition, CdS was introduced into a colloidal montmorillonite suspension and photoredox reactions on the sulfide semiconductor particles were studied.[17] While all of these synthesis methods seek to achieve different aims and use different starting materials, they are all based upon two discrete stages of preparation: (1) an ion exchange process for introducing polycations of cadmium hydrate into mesopores or intergallery regions of the matrix materials and (2) a sulfuration process between the intermediates and gaseous H_2S to convert cadmium hydrous oxide pillars to CdS pillars. Where possible in the production of CdS, it is usual to reduce or avoid the direct handling of hazardous H_2S by using a sulfide such as Na_2S as the sulfur source,[18] a reagent like thioacetamide to release H_2S during reaction,[19] or a single precursor like $Cd(CH_3COS)_2$-(tetramethylethylenediamine) which contains both Cd and S that can produce CdS by thermal decomposition.[20] A properly selected precursor instead of H_2S may be used to prepare the composites of CdS and desired matrixes, and if a scheme is designed to produce the composites by one step instead of the conventional two discrete processes, then a safer and simpler preparation will be realized, which will be an important contribution to the materials research society.

This paper introduces a novel one-step method for the synthesis of CdS/montmorillonite nanocomposites. The simple approach involves a combination of an ion exchange process and an in situ hydrothermal decomposition process of a complex precursor for CdS, so avoiding the need for direct handling of the hazardous H_2S. Moreover, the sizes of the CdS in the composites can be controlled to some extent by varying the amount of the complex preocursor for the synthesis.

2. Experimental Section

Sodium montmorillonite clay (Hithix) from ECC International, Ltd., was used. This clay possessed an average particle size below 2 μm, and its cation exchange capacity is 80 mequiv/100 g clay. The cadmium chloride $CdCl_2$ and thiourea $CS(NH_2)_2$ were supplied by Aldrich and used as purchased. A homogeneous aqueous montmorillonite suspension was prepared such that 1.5 g of the clay was dispersed into 50 mL of deionized water while stirring vigorously. $CdCl_2$ and $CS(NH_2)_2$ of controlled amounts were dissolved into 15 mL of deionized water, and the molar ratio of $CdCl_2$ to $CS(NH_2)_2$ was maintained at 1:2 so as to yield the metal−thiourea complex, $Cd[NH_2CSNH_2]_2Cl_2$, a precursor to CdS upon hydrothermal decomposi-

* To whom correspondence should be addressed. E-mail: zhaohui.han@emu.usyd.edu.au.

† Australian Key Centre for Microscopy and Microanalysis.

‡ School of Chemistry.

10.1021/jp046541i CCC: $30.25
Published on Web 01/20/2005

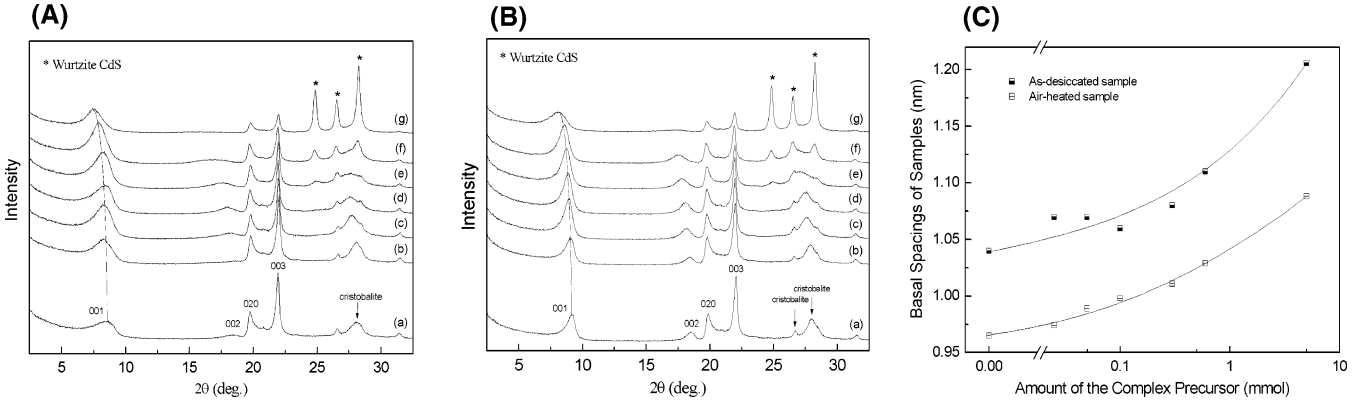

Figure 1. XRD traces of (A) as-desiccated reaction products and (B) corresponding air-heated products, synthesized from the 1.5-g montmorillonite and $Cd[NH_2CSNH_2]_2Cl_2$ complex of various amounts: (a) 0.0, (b) 0.025, (c) 0.05, (d) 0.1, (e) 0.3, (f) 0.6, and (g) 5.0 mmol. (C) Basal spacing of the sample as a function of the complex amount for samples before and after the heat treatment.

tion. This complex precursor solution was then added dropwise to the clay suspension during continuous stirring for 30 min. This starting aqueous suspension was transferred into an 80-mL Teflon lined stainless autoclave and kept at 170 °C for 6 h. Montmorillonite reference material was prepared using the same amount of montmorillonite suspension autoclaved under the same conditions without adding any $Cd[NH_2CSNH_2]_2Cl_2$ complex. For each case, the solid in the resultant mixtures was separated after the reaction by centrifugation and desiccated by vacuum evaporation at ambient temperature. Finally, a portion of each as-desiccated sample was heat-treated at 170 °C in air for 3 h to get the corresponding air-heated sample, to examine the product from a different side.

X-ray diffraction (XRD) was conducted on a Shimadzu XRD-6000 diffractometer equipped with a graphite monochromator. Cu Kα radiation (0.15418 nm) and a fixed power source (40 kV, 40 mA) were used. The data were collected at a scanning rate of 0.5°/min over the 2θ range of 2.5−32.5°, covering the main characteristic diffraction peaks of both the sulfide and the clay. Analytical transmission electron microscopy (TEM) was conducted on a VG HB601 scanning transmission electron microscope where a very bright and coherent electron beam of a 1.0-nm probe diameter was used for elemental analysis. Microanalysis using energy-dispersive X-ray spectroscopy (EDXS) and electron diffraction (ED) was performed on a JEOL JEM-3000F field emission electron microscope under an accelerating voltage of 300 kV, and high-resolution TEM (HR-TEM) images were taken also on this instrument. Conventional TEM was performed on a Philips CM12 electron microscope operating at 120 kV, and the average particle sizes of selected samples were worked out from the particles recorded in the TEM images. The samples used for the particle-size measurements were specially made by the following procedure: centrifuge the reacted suspension to get the solid product, rinse the solid repeatedly using deionized water, and then drop the aqueous suspension of the product onto a holey carbon-coated copper grid. These samples prepared this way will faithfully reflect the true existence state of the particle, because there is no drying and grinding treatment that may change the dispersion state of the particles. Diffuse reflectance UV−visible spectra of the samples were recorded on a Varian Cary 5E UV−vis−nearinfrared spectrophotometer, the scanning range was 200−800 nm, and the reference was barium sulfate. Nitrogen sorption isotherms were obtained on a Quantachrome Autosorb-1 surface area and pore size analyzer; the samples were degassed at 170 °C overnight prior to measurement.

3. Results and Discussion

3.1. Evidences for CdS Pillars in the Reaction Products. The products synthesized from the reaction between the $Cd[NH_2CSNH_2]_2Cl_2$ complex and the montmorillonite in the suspension system were characterized as-desiccated using XRD analyses. Results are summarized in Figure 1A, which provides diffractometry traces of the samples synthesized at 170 °C from the 1.5 g of clay and the complex of various amounts, ranging from 0 to 5 mmol. Inspection of the traces reveals that the montmorillonite $\{001\}_m$ diffraction between 5 and 10° occurs at a progressively lower angle as the amount of the complex increases, toward a minimum value. The enlarged intergallery distance of the clay after reacting with the complex suggests that intercalation process has occurred via ion exchange, and the expansion of basal spacing of the product confirms that there must be something introduced or produced in the intergallery space of the montmorillonite. The pillars are not likely oxides or hydroxides, because they have not been observed in the result produced from the $Cd[NH_2CSNH_2]_2Cl_2$ complex only after the hydrothermal decomposition at such a temperature; instead, the CdS phase was detected as the sole product. Therefore, analogous to general intergallery expansion due to oxide pillars, herein the intergallery expansion of products synthesized by the hydrothermal decomposition of the $Cd[NH_2CSNH_2]_2Cl_2$ complex, the CdS precursor, should be ascribed to the CdS pillars in the samples.

Considering that the products are synthesized from aqueous systems, one may think the intergallery expansion of products is due to the water adsorbed in the intergallery space rather than due to the CdS pillars, because the desiccating process at ambient temperature cannot remove the water completely. To clarify this, the as-desiccated reaction products are heated at 170 °C in air for 3 h to remove the water adsorbed in the samples; such air-heated samples are also characterized by XRD analyses, and the results are presented in Figure 1B. The XRD traces reveal that the $\{001\}_m$ diffraction occurs at a progressively lower angle as the amount of the complex precursor increases, toward a minimum value. The change of the $\{001\}_m$ peak position reveals that the intergallery space of the montmorillonite remains expanded following the heat treatment for all the as-desiccated composite samples. This is significant because it indicates that there are solid species, supposedly the CdS pillars, which are tightly bound in the intergallery layers of the clay, and this would be a natural result of an ion exchange process. The $\{001\}_m$ peak shift reflects the thickness of the CdS pillars. A higher concentration of the $Cd[NH_2CSNH_2]_2Cl_2$ complex leads to a higher equilibrium concentration of the complex in

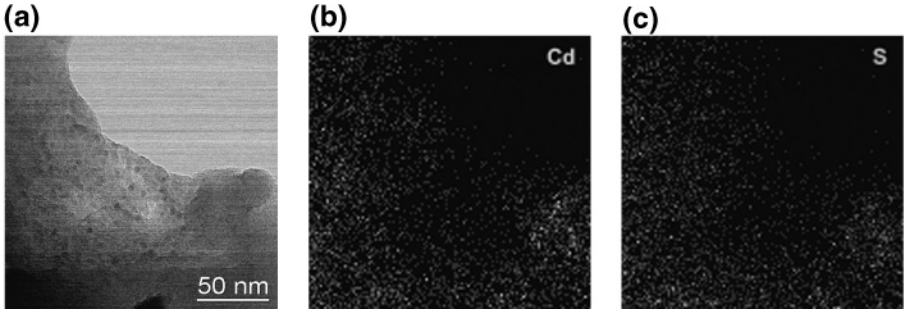

Figure 2. Analytical STEM of an as-desiccated sample: (a) an image of a general region that does not contain CdS nanoparticles, (b) elemental mapping of Cd, and (c) elemental mapping of S.

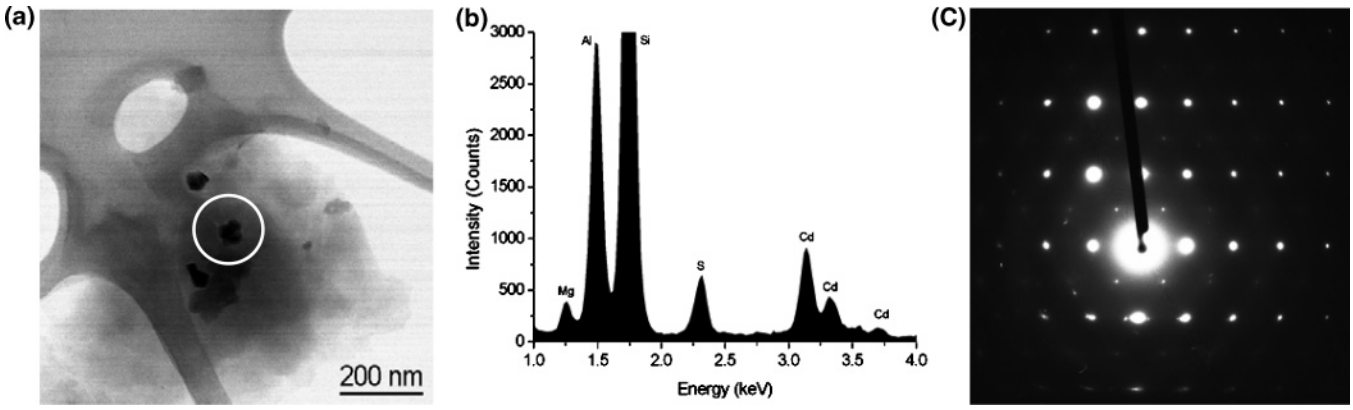

Figure 3. (a) TEM image of a general sample region containing particles of a darker contrast, (b) EDXS of a dark particle in the selected area, and (c) ED pattern of the dark particle.

the intergallery space of the clay, which in turn produces CdS pillars of larger sizes by the subsequent hydrothermal decomposition, expanding the intergallery distance and making the $\{001\}_m$ peak shift toward a lower angle on the XRD pattern. The average sizes of the pillars in the different samples are very small, generally of the order of sub-nanometers.

Compared with the as-desiccated samples, the corresponding air-heated samples have the $\{001\}_m$ peaks systematically shifted to a higher angle, indicating a systematic contraction of intergallery distance. The contraction is expected as a result of the removal of the water adsorbed in the intergallery space of the samples. The change in the basal spacing as a function of the complex amount for as-desiccated and air-heated samples is plotted in Figure 1C. The change of the basal spacing subject to the amount of the complex used for the synthesis demonstrates that the size of the pillars could be controlled to an extent by varying the amount of the complex for the synthesis, although the maximal thickness of the CdS pillars is still very small.

Besides the XRD technique, microscopy and microanalysis could be an alternative technique to identify the pillars in the composites. Because the pillars in the intergallery space of the composites are very thin, the concentration of the pillars is so low that it is below the detecting limits of most conventional electron microscopes. Many attempts have been made; however, it appears that only the analytical scanning TEM (STEM) is sensitive enough to give reasonably convincing results. The analytical results of a representative, the as-desiccated product synthesized from the 1.5-g montmorillonite and 0.6-mmol Cd-$[NH_2CSNH_2]_2Cl_2$ complex, are summarized in Figure 2. The bright-field TEM image providing an overview of a general region of the sample is shown in Figure 2a. The mappings for the distribution of Cd and S in the sample are presented in Figure 2b,c. The presence of the two elements in the main body of the clay supports the conclusion that the expanded basal spacing arises from the pillaring of CdS in the intergallery space because the nanometer electron probe has stimulated discrete signals from Cd and S; the signals generated suggest these species are now intrinsic to the montmorillonite host structure. The faint dots denote weak signals, which are reasonable for the very low content of sub-nanometer CdS pillars in the intergallery space of the composites.

3.2. Evidences for CdS Particles in the Reaction Products. The characteristic diffraction of wurtzite CdS ($P6_3mc$; a = 0.4140 nm, c = 0.6719 nm) is observed in the sample synthesized from the 0.05-mmol Cd$[NH_2CSNH_2]_2Cl_2$ complex, and the diffraction peaks become more apparent in the sample synthesized from a greater amount of the complex, as evidenced in Figure 1A,B. This diffraction is interpreted as the precipitation of CdS nanoparticles outside the intergallery space of montmorillonite. The increasingly sharper diffraction peaks of the CdS suggest that the CdS crystallites with a larger average size are produced when the amount of the complex is increased for the synthesis. This increase is logical simply because more complex precursor feed will be more favorable to the production and crystal growth of the CdS during reaction. On the other hand, less feed of the complex precursor is unfavorable to the crystal growth or even cannot afford CdS nanoparticles; this will explain why there is no CdS diffraction in the sample synthesized from the 0.025-mmol complex, and this feed of the complex is too low to produce CdS nanoparticles with a population that is significant enough to be detectable by the XRD technique.

Microscopy and microanalysis was undertaken focusing on a sample region containing some darker patches, the putative CdS nanoparticles. Figure 3a shows a TEM image providing an overview of the sample. Figure 3b shows the results of EDXS from a darker region (circled in Figure 3a) and demonstrates that there is a high content of CdS precipitates. In this spectrum, besides Cd and S for the CdS, Mg, Al, and Si for the montmorillonite are also presented, as would be expected.

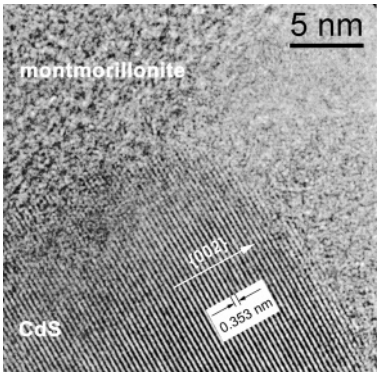

Figure 4. HRTEM image of a CdS grain in the montmorillonite host.

Quantitative analysis reveals that the contents of S in general area are always excessive over those of the Cd, although in some measured region the ratio could be fairly close to 1:1 (48.09 atom % for Cd and 51.91 atom % for S, worked out on the basis of Cd and S only). Figure 3c shows the ED pattern of a single CdS nanocrystallite; the diffraction dots are consistent with the wurtzite CdS crystal of hexagonal symmetry. These microscopy results are unequivocal evidence that the darker particles in the samples are the CdS nanoparticles produced outside of the intergallery space of the clay, which are responsible for the diffraction peaks of the sulfide in Figure 1A,B.

The CdS nanoparticles of the wurtzite structure are also demonstrated by HRTEM of the samples. Figure 4 provides a HRTEM image showing a CdS grain in the composite. The crystalline CdS shows regular projection lines of the {002} crystal plane, and the distance between the crystal planes is 0.353 nm, which is in agreement with the reference data of wurtzite CdS (0.3599 nm, JCPDS PDF-2 database no. 41-1049). The surrounding of the crystalline CdS phase is an amorphous clay phase in the image. The montmorollonite clay layers were crystalline but appeared to be extremely sensitive to the high voltage of the microscope (300 kV was empoloyed in this case), and the crystalline phase was vitrified to an amorphous phase immediately after it was exposed to the electron beam, leaving a distinctive contrast with the crystalline CdS phase surrounded. The CdS of a hexagonal wurtzite structure in the products is desirable if the materials are used as photocatalysts for hydrogen production from water, because the hexagonal CdS has a better activity than the cubic CdS.[12,13]

Consistent with the XRD results, CdS nanoparticles have been rarely observed by TEM in the sample synthesized from the 0.025-mmol complex, because the very limited feed of the complex precursor could not produce many CdS nanoparticles. The particle size of CdS in the sample shows an increase as the amount of complex for the synthesis is increased from 0.05 to 5.0 mmol, following the same trend as the sulfide crystallite size. The changing trend is thought to be a thermodynamic effect because the driving force to precipitate CdS is expected to increase with increasing complex concentration which, in turn, would provide an increased supply of Cd and S to CdS precipitates. This dependence of the CdS particle size on the feed of the $Cd[NH_2CSNH_2]_2Cl_2$ complex suggests that the size control of CdS particles is possbile by varying the amount of the complex for the synthesis.

On the basis of the XRD and electron microscopy and microanalysis, one can conclude that the composites of CdS and montmorillonite, the CdS/montmorillonite, have been synthesized from the montmorillonite clay and the $Cd[NH_2CSNH_2]_2Cl_2$ complex. The acquirement of CdS nanoparticles in the composites makes this work distinctive from previous work that had not obtained CdS nanoparticles in the similar composites synthesized by the conventional method involving a separate sulfuration process. For instance, no nanocrystalline CdS was detected in the composites of CdS and laponite clay, even where the nominal sulfide content reached 0.5 mmol/g clay.[21]

3.3. Proposed Reaction Mechanism to the Composites. The XRD traces evidencing the changes of the $\{001\}_m$ diffraction peak due to CdS pillars and diffraction due to CdS particles, together with the electron microscopy and microanalysis results evidencing the distribution and size of CdS in the products, provide important insights into reaction mechanism to the CdS/montmorillonite nanocomposites. Compared with the conventional synthesis methods that comprise an ion exchanging process and a separate sulfuration process, the synthesis approach introduced here combines the two processes: specifically, the exchange process of the Na^+ cations of the clay with the $Cd[NH_2CSNH_2]_2^{2+}$ cations in the aqueous suspension and the in situ hydrothermal decomposition of the complex precursor at an elevated temperature. The hydrothermal decomposition of the complex in the intergallery space of the montmorillonite produces CdS pillars, while the hydrothermal decomposition of the complex outside of the intergallery space of the montmorillonite, especially in the solution, produces CdS nanoparticles. Therefore, the CdS/montmorillonite was simply synthesized by one step without involving the direct handling of hazardous H_2S. The mechanism to the production of the CdS/montmorillonite nanocomposite in the suspension system involving the montmorillonite clay and the $Cd[NH_2CSNH_2]_2Cl_2$ complex is schematically illustrated in Figure 5.

3.4. UV−Vis Spectra of the Samples. The absorption band of CdS is located in the visible wavelength range, and the absorption shifts to the ultraviolet region as the particle size decreases.[22] Diffuse-reflectance UV−visible spectra were recorded for the as-desiccated samples synthesized from various amounts of the $Cd[NH_2CSNH_2]_2Cl_2$ complex. The spectra in

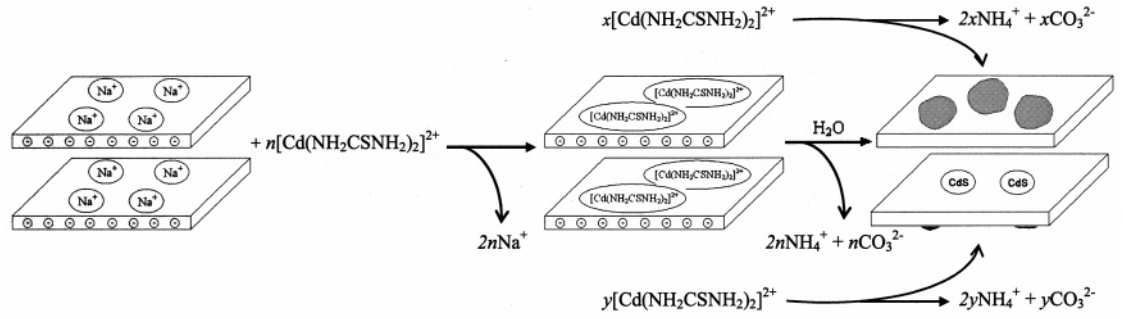

Figure 5. Summary of the mechanism to the production of the CdS/montmorillonite (the dark blocks denote CdS nanoparticles).

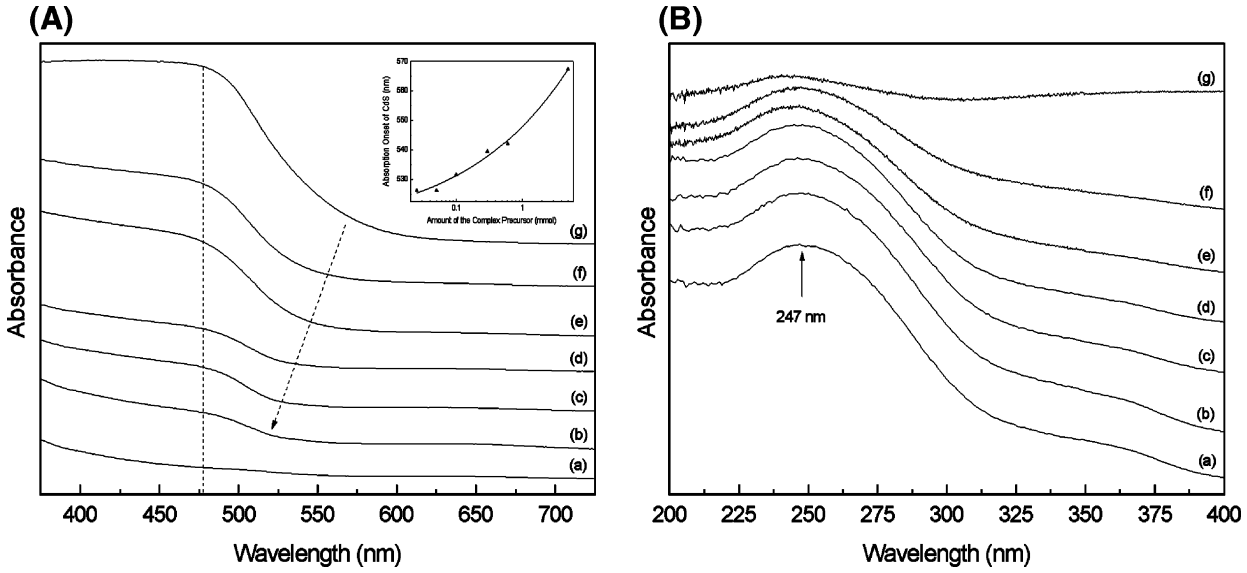

Figure 6. Diffuse-reflectance UV−visible spectra in the range of (A) 375−725 nm and of (B) 200−400 nm for the as-desiccated samples synthesized using the $Cd[NH_2CSNH_2]_2Cl_2$ complex of various amounts: (a) 0.0, (b) 0.025, (c) 0.05, (d) 0.1, (e) 0.3, (f) 0.6, and (g) 5.0. The inset in part A shows the absorption threshold as a function of amount of the complex.

the wavelength range of 375−725 nm emphasizing the close-up of the absorption peaks of CdS nanoparticles are summarized in Figure 6A. Compared with the montmorillonite reference, the nanocomposites show the absorption peaks of CdS and the absorption threshold at 478 nm. As indicated by the arrow, the absorption onset shifts to a lower wavelength as the sulfide concentration in the composite decreases. A plot showing the absorption threshold as a function of the complex amount is presented as an inset in this figure. The shifting trend is consistent with the XRD and TEM results and suggests that smaller CdS nanoparticles are yielded when the concentration of the complex is more dilute. The blue shift of the absorption onset of CdS in the CdS/montmorillonite is comparable to the result observed in the composite of CdS and laponite clay, where the absorption onset exhibited a blue shift when the exchange concentration of Cd was decreased.[21] The spectra in the range of 200−400 nm, which may reveal the absorption peaks of CdS of much smaller sizes, are separately plotted in Figure 6B. It shows that there are no absorption peaks that can be ascribed to CdS species, expect for the peak at 247 nm that is apparently due to the montmorillonite clay. According to the $\lambda_{onset}-2R$ relationship,[23] the sub-nanometer CdS pillars in the CdS/montmorillonite nanocomposites, if they show the absorption, should be below 200 nm and, for this reason, are not observed in our measurement. The samples heated in air at 170 °C for 3 h were also measured for the UV−vis absorption and found to show similar absorption thresholds to the as-desiccated equivalents. This can also be interpreted that the as-desiccated composites remain stable after the heat treatment in air.

3.5. Mesoporous Features of the Samples. Nitrogen ad/desorption isotherms were measured, and these reveal important structural characters of the CdS/montmorillonite nanocomposites. The nitrogen uptakes of the composite materials are substantially lower, compared with that of montmorillonite reference. The small hysteresis of the composite indicates less mesoporosity, suggesting that the CdS nanoparticles occupy the mesopore space, leaving relatively little free volume in the clay. As a result, the CdS particles and the mesopores have similar sizes and mostly are in the range of several to tens of nanometers, consistent with the results obtained from TEM. Because the intergallery distance is generally less than 0.2 nm and the N_2 molecules possess a kinetic diameter of 0.364 nm,

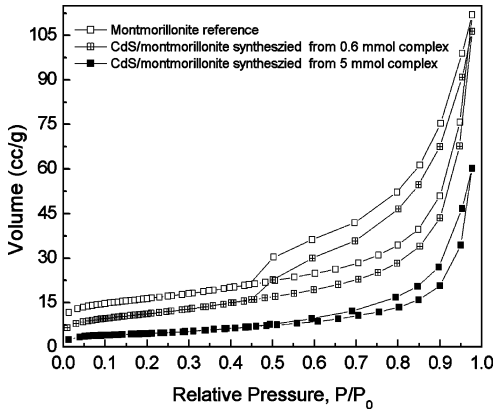

Figure 7. N_2 adsorption isotherms of the montmorillonite reference and two typical CdS/montmorillonite nanocomposites.

the nitrogen molecules could not access the intergallery space and, therefore, the nanocomposites show a smaller specific surface area and pore volume. Figure 7 shows the isotherms for the montmorillonite reference and two typical composite samples synthesized from the 0.6- and the 5.0-mmol complex, respectively. The isotherms of the nanocomposites have a similar shape to the clay reference but are different in surface area and pore volume. It shows that the specific surface area and total pore volume decrease when a larger amount of the $Cd[NH_2CSNH_2]_2Cl_2$ complex was used for the synthesis, and the composite synthesized from the 5.0-mmol complex in these experiments displays the largest difference from the clay reference. According to the nitrogen desorption data, the specific surface area is reduced from 57 m^2/g in the montmorillonite reference to 16 m^2/g in the composite; the corresponding total pore volume is reduced from 0.12 mL/g to 0.07 mL/g. Besides, the pore size distribution is much broader because of agglomerated CdS nanoparticles in the composite.

4. Conclusion

CdS/montmorillonite nanocomposites are synthesized by a one-step method which combines an ion exchange process and an in situ hydrothermal decomposition process of the $Cd[NH_2CSNH_2]_2Cl_2$ complex. The novel synthesis method does not use

any organic solvents, hazardous H_2S, or involve complicated experimental procedures. The procedure is technologically simple and environmentally safe and presents advantages over the conventional synthesis methods that comprise two separate steps which usually involve the handling of H_2S. The resultant composite is composed of sub-nanometer CdS pillars within the intergallery space and nanometer CdS particles outside of the intergallery of the host clay. A larger amount of complex feed results in a higher equilibrium concentration of the complex within the intergallery space as well as outside of the intergallery space, which yields CdS pillars and CdS nanoparticles with larger sizes. Therefore, the sizes of both the sulfide species are controllable simply by varying the complex used for the synthesis. The CdS nanoparticles in the composites adopt a hexagonal wurtzite structure. The absorption blue shift of the CdS particles in the composites was observed to increase for decreasing CdS particle size.

The CdS/montmorillonite nanocomposites are expected to be useful for various applications, for instance, as photocatalysts for hydrogen production from water. The synthesis method reported here for the CdS/montmorillonite nanocomposites would also seem to lend itself to the production of composites of other clays, such as laponite, saponite, and hectorite, so possessing various structures and properties, which can be optimized for specific applications. These synthesis and characterization experiments are underway, and the results will be reported elsewhere.

Acknowledgment. This work is supported partially by the Australian Research Council (ARC). Dr. Han and Dr. Zhu acknowledge the ARC for APD and QE II Fellowships, respectively. The authors are in debt to Dr. Wei Xing, ARC Centre for Functional Nanomaterials, the University of Queensland, who has kindly offered important technical support. The facilities and scientific and technical assistance from staff in the NANO Major National Research Facility at the University of Sydney are acknowledged gratefully.

References and Notes

(1) Zhang, Q. M.; Li, H.; Poh, M.; Xia, F.; Cheng, Z. Y.; Xu, H.; Huang, C. *Nature* **2002**, *419*, 284.
(2) Lakes, R. S.; Lee, T.; Bersie, A.; Wang, Y. C. *Nature* **2001**, *410*, 565.
(3) Waku, Y.; Nakagawa, N.; Wakamoto, T.; Ohtsubo, H.; Shimizu, K.; Kohtoku, Y. *Nature* **1997**, *389*, 49.
(4) Schwerzel, R. E.; Spahr, K. B.; Kurmer, J. P.; Wood, V. E.; Jenkins, J. A. *J. Phys. Chem. A* **1998**, *102*, 5622.
(5) Sapra, S.; Nanda, J.; Sarma, D. D.; Abed El-Al, F.; Hodes, G. *Chem. Commun.* **2001**, 2188.
(6) Arora, M. K.; Sinha, A. S. K.; Upadhyay, S. N. *Ind. Eng. Chem. Res.* **1998**, *37*, 3950.
(7) Shangguan, W.; Yoshida, A. *J. Phys. Chem. B* **2002**, *106*, 12227.
(8) Arora, M. K.; Sahu, N.; Upadhyay, S. N.; Sinha, A. S. K. *Ind. Eng. Chem. Res.* **1999**, *38*, 2659.
(9) Wang, S.; Choi, D. G.; Yang, S. M. *Adv. Mater.* **2002**, *14*, 1311.
(10) Zhang, Z.; Dai, S.; Fan, X.; Blom, D. A.; Pennycook, S. J.; Wei, Y. *J. Phys. Chem. B* **2001**, *105*, 6755.
(11) Cao, H.; Xu, Y.; Hong, J.; Liu, H.; Yin, G.; Li, B.; Tie, C.; Xu, Z. *Adv. Mater.* **2001**, *13*, 1393.
(12) Arora, M. K.; Sahu, N.; Upadhyay, S. N.; Sinha, A. S. K. *Ind. Eng. Chem. Res.* **1999**, *38*, 4694.
(13) Arora, M. K.; Sahu, N.; Upadhyay, S. N.; Sinha, A. S. K. *Ind. Eng. Chem. Res.* **1998**, *37*, 1310.
(14) Pinnavaia, T. J. *Science* **1983**, *220*, 365.
(15) Burch, R., Ed. *Pillared Clays*, *Catalysis Today*; Elsevier: New York, 1988; Vol. 2−3.
(16) Sychev, M.; de Beer, V. H. J.; Kodentsov, A.; van Oers, E. M.; van Santen, R. A. *J. Catal.* **1997**, *168*, 245.
(17) Enea, O.; Bard, A. J. *J. Phys. Chem.* **1986**, *90*, 301.
(18) Yang, C. S.; Awschalom, D. D.; Stucky, G. D. *Chem. Mater.* **2002**, *14*, 1277.
(19) Zeng, J.; Yang, J.; Zhu, Y.; Liu, Y.; Qian, Y.; Zheng, H. *Chem. Commun.* **2001**, 1332.
(20) Schmid, G. *J. Mater. Chem.* **2002**, *12*, 1231.
(21) Stramel, R. D.; Nakamura, T.; Thomas, J. K. *Chem. Phys. Lett.* **1986**, *130*, 423.
(22) Henglen, A. *Chem. Rev.* **1989**, *89*, 1861.
(23) Wang, Y.; Herron, N. *Phys. Rev. B* **1990**, *42*, 7253.